

Pitfalls Associated with the Estimation of Radiological Burdens on Population Caused by Radiation Accidents

Petr Pecha*, Emilie Pechova**

*Institute of Information Theory and Automation, Prague 8, Czech Republic
(Tel: +420 2 66052009; e-mail: pecha@utia.cas.cz).

**Institute of Nuclear Research, Div. EGP, 250 68 Rez near Prague, Czech Republic

Abstract: The initial intention of this essay was to compare our environmental code PRIMO with the commonly accepted code COSYMA. All basic output radiological variables are in very good agreement after our careful mutual tuning of all input parameters of both products. However, a certain disproportion was encountered when proceeding to the estimation of radiation doses. It became apparent that due to the hidden variability of the parameters of the dosimetric model, the estimation of the radiological impact on the human body can be generated with a different degree of conservatism. These effects should be accounted for when using the environmental codes for assessment of the radiological impact on a population. An alternative approach of the assessment taking into consideration the variability and subsequently uncertainty of the input parameters can afford more informative answers to the evaluation questions. From this point of view, the PRIMO algorithm follows the research trend of progress from the deterministic calculations towards the probabilistic approach of the consequence estimation.

Keywords: Radioactive discharges, consequence assessment, irradiation doses, variability, uncertainty.

1. INTRODUCTION

The environmental program product HARP (HARP, 2012) includes segmented Gaussian algorithms in the PRIMO and SGPM modifications. The latter version can respect time and spatial weather changes. The complicated scenario of the release dynamics is thus synchronized with the available meteorological forecasts. The SGPM is aimed at detailed modelling in the data assimilation procedures (ASIM, 2013). In the following tests we are using the simpler PRIMO component for description of straightforward radioactivity propagation in the air prospectively proposed for the fast sensitivity analysis and "worst case" studies. The safety studies are also incorporated in the EIA Reports within the licensing process when the operational safety should comply with the obligatory governmental regulations.

The aerial transport of the discharged radionuclides is studied here up to 100 km from a source of pollution. The dispersion, deposition and successive radioactivity migration towards the human body is simultaneously modelled. Due to the limited extent of this article the ingestion pathway and the other late-phase consequences are not included here - more can be found online in (HARP, 2012).

Both algorithms are designed consistently in a conservative way. Alternative options for the input model parameters and incorporated transport submodels are interactively offered. This approach leads to the possibility of conservative estimations of the radiation doses now having the character of the *potential* values. The users have a wide range of

possibilities to re-enter the scenario input values from detailed interactive input panels. It could be used especially in cases when the generated output values were gradually coming into conflict with the regulatory limits. Unfortunately, an accidental release scenario is burdened with large uncertainties (release source term, initial plume buoyancy, variability of geographic characteristics etc.). Then, the final assessment procedure can be distorted by the incorporated uncertainties or an ill-defined scenario. The pragmatic solution usually resides in the utilisation of a certain generic assessment code which could quickly and easily generate preliminary "golden mean" (usually optimistic) results. This fast initial guess can be useful at least for the determination of the so-called *expected* values, unfortunately without any information related to the degree of conservatism. If it becomes apparent that the consequences could be serious, attention should be focused on the more detailed evaluation of the potential risk values. Instead of the common generic input values, more convenient site-specific and release type specific values should be found. This problem will be pointed out in the course of the following comparative analysis.

2. VALIDATION PROCEDURE

The PRIMO algorithm splits the whole real radioactivity release into a certain number of time segments, each having its own constant homogenous release rate. For purposes of the "worst case" analysis the same most adverse weather conditions are selected in all time segments and the resulting effects are superimposed. The European product COSYMA

has been chosen for the comparative analysis as the reference code. The product is based on the same family of the dispersion models and works on the assumptions of Gaussian modelling.

2.1 Choice of an accidental radioactivity release scenario

Design basis accident SBLOCA (Small-Break Loss-of-Coolant Accident) initiated by a hypothetically rupture of the instrumentation pipe penetrating through WWER-440 hermetic zone is analysed in (Junek et al., 2008). The instrumentation pipe serves to the sampling of the active water from the pressuriser. The outflow of this small break is in a range of 3 – 5 kg.s⁻¹. The most adverse sequence of the consecutive events was taken into account. Continued cooling of the reactor core during a SBLOCA requires depressurisation of the primary coolant system. Several control interventions follow with the goal of minimising the release of radioactivity out of the hermetic zone. The detailed thermal-hydraulics analysis of the transient processes for the SBLOCA was performed with the assistance of the RELAP code. It led to the time segmentation shown in Table 1.

Table 1. Transient events of SBLOCA scenario

Time (s)	Transient events
0- 1208	Rupture of the pipe for sampling of active water from pressuriser; leaking of active water out of hermetic zone; refilling of IO
1208 – 3906	Leaking continues, start of high pressure pump for IO refilling
3906 - 4137	Leaking continues; IO refilling continues; fast shutdown of reactor and 2 turbogenerators
4137 - 5696	Leaking and refilling continues; auxiliary IO cooling through IIO (SDA); end of leaking from IO at time 5696 s
5696 - 7496	Auxiliary cooling down of IO through IIO (SDA) - termination at 7496 s ; transition of auxiliary cooling to reduction station

IO, IIO – primary and secondary circuit of a reactor

SDA – Steam Dump to the Atmosphere

The activity discharges from IO into the atmosphere were determined for the first four time segments on the basis of the event segmentation from Table 1. The preliminary calculations using the PRIMO code allowed selection of a limited subset of 42 nuclides having a non-negligible contribution to the estimated effective 7-day dose. For purposes of the following comparative benchmark we have reduced the discharges from all four segments into one equivalent segment with a one-hour duration (in Table 2).

Table 2. Modified source term of SBLOCA - instrumentation pipe rupture

nuclide	equivalent 1-hour discharge (Bq.h ⁻¹)	contribution to 7-d eff. dose (%)
¹³¹ I	7.27E+11	35.6
¹³³ I	2.81E+12	30.8
¹³² Te	1.72E+12	10.6
¹³⁵ I	2.34E+12	9.5

¹³² I	2.25E+12	2.2
¹³⁴ Cs	4.15E+10	1.4
¹³⁶ Cs	6.48E+10	1.3
¹³³ Xe	3.15E+13	0.5
⁸⁸ Kr	1.23E+12	0.4
....

2.2 Adjustment of the joint common input parameters

The default values of the mutual input parameters in both codes should be adjusted carefully and with caution. The PRIMO is a live code with guaranteed maintenance. The necessary changes required by a somewhat simpler COSYMA structure can be temporarily incorporated in the PRIMO with fast response thus enabling a satisfactory tuning of the inputs for both codes. The input parameters of the atmospheric, deposition and dosimetric submodels have been adjusted as closely as possible to:

<i>NPP location:</i>	Dukovany
<i>Surface elevation:</i>	flat terrain
<i>Surface roughness:</i>	defaults
<i>Landuse category:</i>	grass (uniform surface)
<i>Dispersion coefficients:</i>	rough terrain
<i>Atmospheric stability category:</i>	D
<i>Wind speed:</i>	3 m.s ⁻¹
<i>Wind direction:</i>	NE
<i>Discharge duration:</i>	1 hour
<i>Wind profile exponent (D cat):</i>	0.34 (cat D)
<i>Buoyant plume rise:</i>	zero
<i>Near-standing building effect:</i>	neglected
<i>Rain during plume passage:</i>	0 mm.h ⁻¹
<i>Aerosol size:</i>	1 μm
<i>Effective dose option</i>	ICRP-60
<i>Dry deposition velocities</i>	see Table 3

Table 3. Dry deposition velocities (m.s⁻¹) for various physical-chemical forms of discharges and landuse categories (for fully developed plant canopy)

Landuse category	Aerosol (1 μm / >1 μm)	Elemental form	Org. bounded
1:urban	0.0005/0.0008	0.005	0.00005
2:grass	0.0015/0.0025	0.015	0.00015
3:agricultur.	0.002/0.003	0.020	0.0002
4:forest	0.0075/0.0085	0.073	0.001
5:water	0.0007/0.0008	0.001	0.0005

3. COMPARISON OF RESULTS

The accident consequences cover a wide range of various individual and collective doses on population and serve as a tool for testing the effectiveness of the countermeasures launched for population protection. But the correct determination of the dispersion in atmosphere and deposition of radioactivity on the ground is an imperative prerequisite. In other words, an errorless functionality of the algorithm should be proved.

3.1 The structure of the generated output values

The dispersion and deposition calculations generate for each nuclide n the set of four fundamental quantities fully describing the release phase $t < 0$; T_{end} , $(T_{end} -$ the radioactive cloud already subsided over the terrain):

- $CAP^n(r, \varphi, z; t)$ - activity concentration in the air (Bq.m^{-3}) (spatial distribution around the source in the computational polar nodes),
- $TIC^n(r, \varphi, z=0; T_{end})$ - time integral up to T_{end} of the near-ground activity concentration in the air (Bq.s.m^{-3}) during the release phase (spatial distribution),
- $DEP^n(r, \varphi, z=0; T_{end})$ - activity deposited on the ground (Bq.m^{-2}) (spatial distribution) during the period $< 0; T_{end}$,
- $TID^n(r, \varphi, z=0; T_{end})$ - time integral up to T_{end} of the activity deposited on the ground (Bq.s.m^{-2}).

On the basis of these values the overall estimation of the radiological consequences is carried out. The doses and committed doses for the external and internal irradiation related to the end of the release (early doses) can be easily generated by a simple multiplication by the constants comprising the corresponding dose conversion factors.

Specifically, the committed dose D_{inh} (Sv) on organ o ($o = 1$ for effective dose) from the inhalation pathway of radionuclide n (50 years for adults, 70 years for children) is determined according to the scheme (related to the T_{end}):

$$D_{inh}^{a,n,o}(r, \varphi, z=0) = TIC^n(r, \varphi, z=0; T_{end}) \cdot u_{inh}^a \cdot F_{inh}^{a,n,o} \quad (1)$$

where TIC is the time integral of the near-ground activity concentration in the air above the location $(r, \varphi, z=0)$, u is the breathing rate for the age category a ($\text{m}^3 \cdot \text{h}^{-1}$), F is the tabulated dose conversion factor for inhalation (Sv.Bq^{-1}). Similarly, the early phase doses D_{gr} (Sv) from activity deposited on the ground (related to the T_{end}) are given by:

$$D_{gr}^{n,o}(r, \varphi, z=0) = TID^n(r, \varphi, z=0; T_{end}) \cdot F_{gr}^{n,o} \quad (2)$$

where F_{gr} is the tabulated dose conversion factor for the groundshine of radionuclide n ($\text{Sv.m}^2 \cdot \text{Bq}^{-1} \cdot \text{s}^{-1}$). The late phase groundshine doses at time T after the release ceased is given by superposition of (2) and the term:

$$D_{2gr}^{n,o}(r, \varphi, z=0) = F_{gr}^{n,o} \int_0^T DEP^n(r, \varphi, z=0; T_{end}) \cdot \exp(-\lambda^n \cdot t) \cdot dt \quad (3)$$

Furthermore, a special algorithm has been developed in (Pechá and Pechová, 2013) for the fast calculation of the cloudshine doses based on the photon fluency rates from the spatial distribution $CAP^n(r, \varphi, z)$ at near distances from the source. Otherwise, the common approximation of submersion into the semi-infinite cloud is applied at larger distances according to (related to the T_{end}):

$$D_{cloud}^{n,o}(r, \varphi, z=0) = TIC^n(r, \varphi, z=0; T_{end}) \cdot F_{cloud}^{n,o} \quad (4)$$

where F_{cloud} is the tabulated dose conversion factor for cloudshine of the radionuclide n on organ o ($\text{Sv.m}^3 \cdot \text{Bq}^{-1} \cdot \text{s}^{-1}$).

3.2 Approval of the main driving quantities

All output radiological values such as irradiation doses in the early or late stages of the accident, countermeasure

estimation, long-term evolution of the specific activities in the agricultural products and food ban effectiveness examination, long-term doses from resuspension etc. can easily and directly be derived from the four main driving quantities. Consequently, the critical issue of the examination of the COSYMA \times PRIMO conformity consists in the investigation of an agreement between the corresponding CAP, TIC, DEP and TID spatial fields. After adjustment of the joint common input parameters described in subsection 2.2 the TIC fields are illustrated in Fig. 1a for 3 selected physical-chemical forms of the discharged radionuclides.

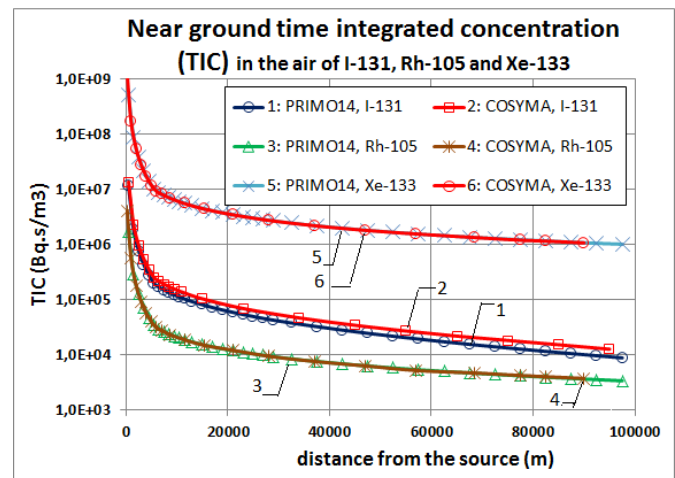


Fig. 1a. Time integral of the near-ground activity concentration in the air (^{133}Xe – noble gas, ^{131}I – elemental form, ^{105}Rh – aerosol).

The radioactivity deposited on the ground is demonstrated in Fig. 1b for ^{131}I (elemental form) and ^{132}Te (aerosol).

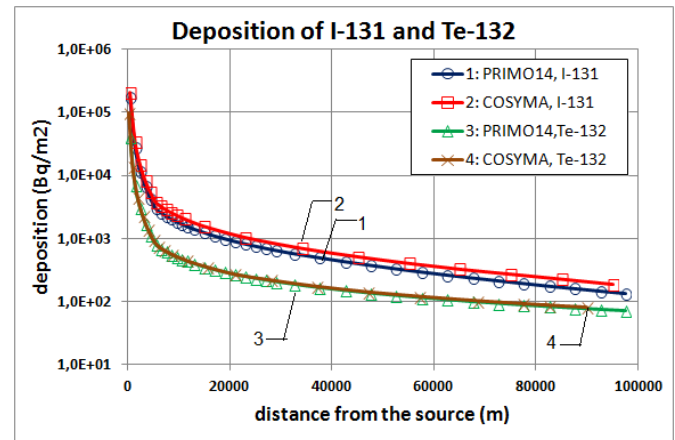


Fig. 1b. Activity deposited on the ground just after the radioactive cloud subsided (^{131}I – elemental, ^{132}Te – aerosol).

3.3 Doses of irradiation inferred from the main driving quantities

The figures 1a and 1b give good evidence of the COSYMA \times PRIMO agreement. Therefore, we expected good agreement between other entities, too. The committed 7-day effective dose for adults was generated and displayed in Fig. 2. In spite

of the same effective dose option according to ICRP-60 declared in both products, the correspondence of the results is rather poor and should be clarified. With regard to expression (1), the reason for this discrepancy must reside in the particular values of the conversion factors F_{inh} .

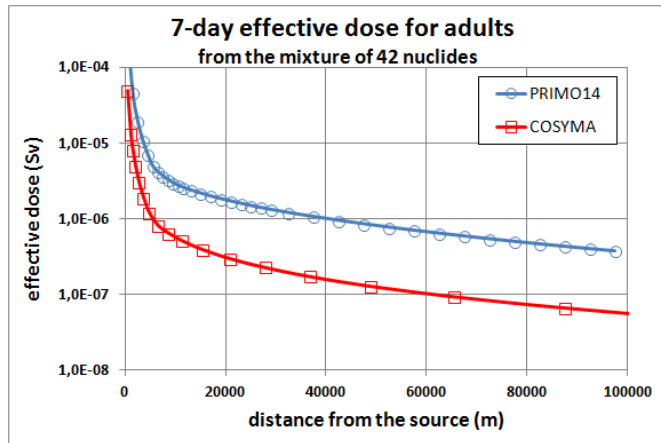


Fig. 2. Committed effective dose for adults (cloudshine, groundshine, inhalation; no ingestion) after 7 days from the SBLOCA release.

First of all we shall stress the peculiar features contained in the recipe how to construct (select) the suitable values of F_{inh} . The publication (FGR13, 1998) points to the uncertainties in a biokinetics model, on the basis of which the conversion factors for inhalation are determined. The form of the inhaled material is classified in terms of the rate of absorption from the lungs into the blood, using the classification scheme of ICRP. The types F, M and S represent fast, medium and slow rates. According to (FGR13, 1998): “ICRP recommends default absorption types of most of the radionuclides, but information underlying the selection of an absorption type is often very limited and in many cases reflects occupational rather than environmental experience. Due to uncertainties in the form of a radionuclide likely to be inhaled by members of the public, various plausible absorption types have been addressed in the derivation of the risk coefficient for inhalation of a radionuclide”. FGR13(1998) explicitly states that airborne activity is in the particulate form. The risk coefficients for inhalation are based on the activity median aerodynamic diameter (AMAD) of 1 μm .

The exceptions are given here for example for iodine which can be either in the form of a vapour (type V), or a gas (methyl iodide CH_3I , type G) or a particulate (type F or type M). Tellurium can be assumed in the form of a vapour (type V) or a particulate (type F, type M, type S). The selection for computation is not given unambiguously and expert judgement resulting from these characteristics of the activity release scenario is inevitable. It is evident that construction of a database of the conversion coefficients for inhalation in either code is somewhat different:

- PRIMO follows Table No. 6 from the obligatory Regulation (2002) (corresponds to ICRP 60), where the dose conversion factors for inhalation are recommended (see extract in Table 3 here). For a specific type of the release scenario, an ambiguity of choice among the types F, M, S should be handled with help of an external expert

consultant. If no information is available, we use the worst value among the F, M and S types. The conservative values for type V for iodine are taken from Table No. 7 of the obligatory Regulation (2002). PRIMO database leads to generation of conservative potential values.

- The COSYMA approach also declares the use of effective dose option according to ICRP-60. But selection of the lung type is simplified: “.... reduction to only one lung class (the values referring to oxides are taken) and one age group (adults)” (Hasemann I., 1994). Lung clearance type V is not assumed at all. The database has a generic character leading to the generation of rather average expected values.

The above-mentioned conclusions reveal the discrepancy from Fig. 2 between both codes. The partial model experiment for confirmation of the assertion is illustrated in Fig. 3. The radionuclide ^{131}I having the highest contribution to the 7-d effective dose is assumed alone. The conversion coefficients are summarised in Table 4.

The calculation of 7-day committed effective dose for adults for the only nuclide ^{131}I has been run twice with values of F_{inh} equal to 2.0E-9 and 7.4E-9 (Sv.Bq-1). The results are displayed in Fig. 3. Curves 2 and 3 nearly coincide when the value of the conversion coefficient is changing from the type V to the (generic) type S.

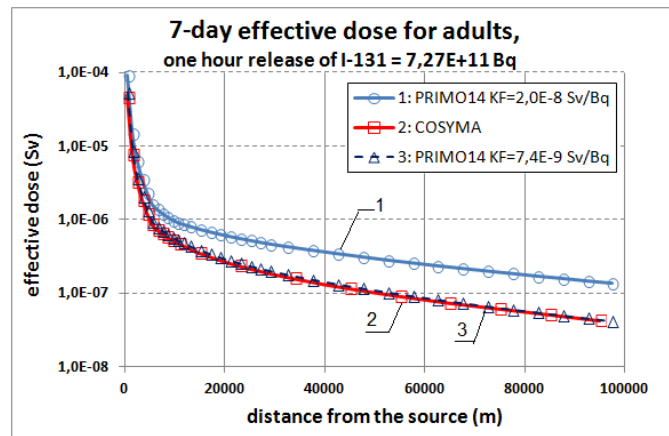


Fig. 3. Committed effective dose for adults (cloudshine, groundshine, inhalation; no ingestion) after 7 days from the release. The contribution of only ^{131}I nuclide is assumed.

Table 4. Effective dose conversion factors for inhalation (Sv.Bq⁻¹) for ^{131}I applied in the code PRIMO

lung type	age <1year	<1,2> years	<2,7> years	<7,12> years	<12,17> years	adults
F	7.2E-8	7.2E-8	3.7E-8	1.9E-8	1.1E-8	7.4E-9
M	2.2E-8	1.5E-8	8.2E-9	4.7E-9	3.4E-9	2.4E-9
S	8.8E-9	6.2E-9	3.5E-9	2.4E-9	2.0E-9	1.6E-9
V ⁽¹⁾	1.7E-7	1.6E-7	9.4E-8	4.8E-8	3.1E-8	2.0E-8
V ⁽²⁾	1.3E-7	1.3E-7	7.4E-8	3.7E-8	2.4E-8	1.5E-8

⁽¹⁾ ^{131}I - elemental form; ⁽²⁾ ^{131}I - methyl iodide

3.4 An example of accounting for the site-specific input data

The local characteristics of the surface coverage and elevation are expressed in a discrete form on the polar computational grid. The calculated area is divided into the 16 directions of the windrose and 35 radial distances from the source of pollution up to 100 km: (5)

1, 2, 3, 4, 5, 6, 7, 8, 9, 10, 11, 12, 14, 16, 18, 20, 22, 24, 26, 28, 30, 35, 40, 45, 50, 55, 60, 65, 70, 75, 80, 85, 90, 95, 100

The discretisation is introduced for the superficial input fields of the surface elevation and surface roughness, surface landuse characteristics, gridded demographical data and potentially for the local rain areas. For each subarea of the polar grid the prevalent categories of the quantities are determined. Depletion of the radioactivity in a plume during its propagation over the terrain is caused by removal mechanisms of radioactivity decay and dry and wet activity deposition. Release source strength A (Bq.s⁻¹) at distance x of the plume propagation is depleted according to (6)

$$A^n(x, y=0, z=h_{ef}) = A^n(x=0, y=0, z=h_{ef}) \cdot f'_R(x) \cdot f'_F(x) \cdot f'_W(x)$$

where $f'_R(x)$, $f'_F(x)$, $f'_W(x)$ are fractions of activity depleted (dissipated) out of the cloud during its propagation from the release point up to the distance x . The removal processes of dry and wet deposition depend on physical-chemical forms of admixtures and land-use characteristics of the terrain. More details, e.g., in (Pechá et al., 2007).

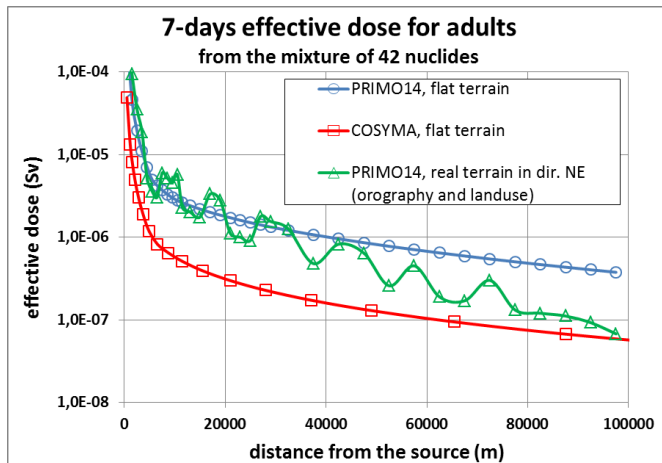


Fig. 4. Realistic modelling on the real terrain. Scenario SBLOCA, propagation in NE (North-East) direction.

The results for the SBLOCA scenario for the case of the flat terrain and uniform landuse type 2 (grass – see Table 3) are illustrated in Fig. 2. Now we shall recalculate the scenario for the straight-line propagation in direction 3 (NE – North-East) around the real NPP Dukovany. In addition to the radial distances (5) the following landuse types (categories according to Tab. 3) are prevalent on the consecutive polar net segments in the NE direction: (7)

3 4 4 4 3 3 4 4 4 3 3 3 4 4 4 3 4 4 3 4 3 3 3 3 3 3 3 3 3

The third curve is included in Fig. 2 and all is shown in Fig. 4. The new standalone results for the real terrain are also demonstrated in 2-D in Fig. 5. Only categories 3 (agri) and 4 (forest) are found in the NE direction. The terrain has more

“deposition potency” than the original uniform type for grass. It results in a deeper progress of the third curve with higher values near the source and lower ones at distances closer to the end. The peak values correspond to the higher deposition in the forest areas and have a real meaning.

7-day committed effective dose for adults - straight-line propagation. Dir. NE, 3 m/s, Pasquill stability category D

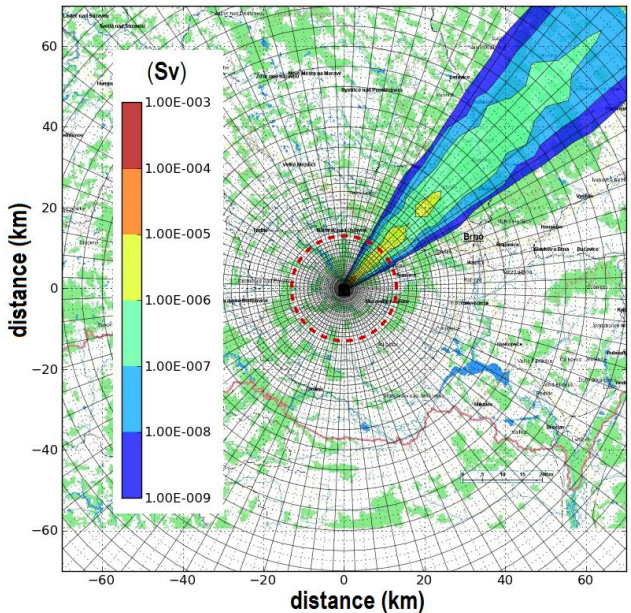


Fig. 5. Scenario SBLOCA: 2-D image (complementary to 1-D graph in Fig. 4) of realistic modelling on the real terrain on the map background around NPP Dukovany (automatic output from the HARP visualisation subsystem).

The above-mentioned facts support significance of the customization of the estimation tools on the local conditions of a nuclear facility. The effects are somewhat exaggerated because they are related to the fully developed plant canopy.

4. TRENDS IN CONSEQUENCE ASSESSMENT METHODOLOGY

According to the current aim of the calculations, either expected (best estimate) set or conservative (potential) input data files are formulated. The partial runs can have the character of sensitivity studies or “worst case” analysis. However, the input options cannot be arbitrary and must follow the internal attributes of the permissible values. An alternative statistical methodology complying with the inherent uncertain character of the task introduces a measure of confidence in the model predictions.

We have to distinguish between *variability* and *uncertainty* of a certain variable. Variability reflects changes of a certain quantity over time, over space or across individuals in the population. The variability represents diversity or heterogeneity in a well-characterised population. The term “uncertainty” covers the stochastic uncertainties, the structural uncertainties representing partial ignorance or incomplete knowledge associated with lack of perfect information about poorly-characterised phenomena or

models, an uncertain (ill-defined) release scenario or the input model uncertainties.

Recent trends in the risk assessment methodology insist on transition from deterministic procedures to the probabilistic approach which enables to us generate more informative probabilistic answers on the assessment questions. The quantitative reliability statements can determine a *level of confidence* with regards to exceeding the postulated limits and then provide a much firmer basis for qualitative statements in the field of emergency management. The probabilistic tool offers support related to the estimation of conservatism or adequacy of results.

The COSYMA code declares two run options: deterministic and probabilistic. In our opinion, its probabilistic run is WVA (Weather Variability Assessment) belonging to a special application from the domain of PSA-Level 3 analysis, rather than a “full - blooded” probabilistic approach. We have performed an extensive WVA in (Hofman et al., 2011). The variability of meteorological inputs represented by historical long sequences of the archived values (for each hour in the years 2008 and 2009: 17520 sequences) has been processed. The consequences determined from a distribution of the meteorologically based samples of the output values were processed statistically.

The perception of distinction between variability and uncertainty of the meteorological inputs is crucial. Seasonal and diurnal changes result in variability in meteorological data and their statistical processing provides certain information related to the averaged (weighted) values. Unlike this, the uncertainty analysis and assimilation procedures are always related to a *particular moment of an accident initiation*. The meteorological situation related to the specific time of release is given by superposition of the nominal values (measurements or forecasted for that moment) and random fluctuations due to the stochastic nature of the turbulent processes in the atmosphere.

5. CONCLUSIONS

The early stage of a radiation accident has been verified with help of the PRIMO code. This code can be used by the potential authorised contracting authorities planning the construction and operation of a nuclear facility when compliance with the strict obligatory governmental regulations has to be proved. The product was submitted to the Czech Standardisation Board and approved (2013) for its use in the field of nuclear safety. The “worst case” analysis should be performed for a set of prescribed Design Basis Accidents (one of them was the SBLOCA examined here). Before using PRIMO, one must be aware of all pitfalls of the assessment and undertake responsibility for delivery of the relevant input data and correct interpretation of the results. The variations of the inputs should be adjusted with regard to the parameter distributions. In the simplest case the interval of the potential minimum and maximum values based on the expert elicitation procedures can be assumed. If the parameter is assumed to be random, the values should be sampled from its probability density function. We are thus entering the area of the sensitivity and uncertainty studies and up-to-date

trends of the probability approach can be followed. The HARP code is designed for either deterministic or probabilistic analysis (HARP, 2013). Simulation of the uncertainty propagation through the model also provides a basis for another main task of the analysis called assimilation of the model predictions with the real measurements coming from the terrain. Data assimilation represents the way to progress from a model to reality and can substantially improve the quality of the model predictions (ASIM, 2012).

ACKNOWLEDGEMENT

This research was supported by the Czech-Norwegian research program, project 7F14287 STRADI.

REFERENCES

- ASIM(2012): ASIM - A software Tool for Assimilation of Model Predictions with Observations from Terrain. URL: <http://asim.utia.cas.cz/>
- FGR13 (1998): Helth Risks from Low-Level Environmental Exposure to Radionuclides. *Federal Guidance Report No. 13, Part I.*
- HARP(2013): HARP - HAzardous Radioactivity Propagation: A Software Tool for Fast Assessment of Radiological Consequences of Radiation Accident URL: <http://havarpp.utia.cas.cz/harp/>
- ICRP(2012): Compendium of Dose Coefficient based on ICRP Publication 60. *Annals of the ICRP*.
- Junek, V., Pechova, E. , Kelemen, R., and Pecha, P. (2008). Radiological Consequences of the Instrumentation Pipe rupture for reactor WWER-440. *Report EGP 5014-F-080066*.
- Hasemann I. and Ehrhardt, J. : COSYMA: Dose Models and Countermeasures for External Exposure and Inhalation. *KfK 4333*.
- Hofman, R., Pecha, P. (2011): Application of regional envir. code HARP in the field of off-site consequence assessment, *Proc.of PSA2011*, Wilmington, USA. URL: http://havarpp.utia.cas.cz/harp/report_PDF/2011/PSA_2011.PDF.
- Pecha, P., Hofman, R. and Pechová, E. (2007): Training simulator for analysis of environmental consequences of accidental radioactivity releases, *Proc. of the 6th EUROSIM Congress on Modelling and Simulation, Ljubljana, SI*.
- Pecha, P. and Pechova, E. (2014). An unconventional adaptation of a classical Gaussian plume dispersion scheme for the fast assessment of external irradiation from a radioactive cloud. *Atmospheric Environment, Volume 89, June 2014, pages 298-308.* URL: http://havarpp.utia.cas.cz/harp/Photon_fluence.PDF.
- Regulation (2002): Radiation protection. *Regul. 307/2002 Sb. of the State Office for Nucl. Safety, Czech Republic.*